

A low noise thermometer readout for ruthenium oxide resistors

D. J. Fixsen^{a)} and P. G. A. Mirel

SSAI Code 685, NASA/GSFC Laboratory for Astronomy and Solar Physics, Greenbelt, Maryland 20771

A. Kogut

NASA/Goddard Space Flight Center, Laboratory for Astronomy and Solar Physics, Greenbelt, Maryland 20771

M. Seiffert

Jet Propulsion Laboratory, California Institute of Technology, 4800 Oak Grove Drive, Pasadena, California 91109

(Received 21 May 2002; accepted for publication 7 July 2002)

The thermometer readout and thermal control system for the Absolute Radiometer for Cosmology, Astrophysics, and Diffuse Emission (ARCADE) experiment is described, including the design, testing, and results from the first flight of ARCADE. The noise is equivalent to about 1Ω or 0.15 mK in a second for the RuO_2 resistive thermometers at 2.7 K . The average power dissipation in each thermometer is 1 nW . The control system can take full advantage of the thermometers to maintain stable temperatures. Systematic effects are still under investigation, but the measured precision and accuracy are sufficient to allow measurement of the cosmic background spectrum. © 2002 American Institute of Physics. [DOI: 10.1063/1.1505108]

I. INTRODUCTION

The Absolute Radiometer for Cosmology, Astrophysics, and Diffuse Emission (ARCADE) experiment¹ is designed to detect or limit spectral distortions in the Rayleigh–Jeans tail of the Cosmic Microwave Background. The key to this experiment is the external calibrator. The absolute temperature of the calibrator is required to compare to other experiments such as Far InfraRed Absolute Spectrophotometer (FIRAS).^{2,3} It is more critical, however, that the calibrator be isothermal and remain at a constant temperature while it is shifted between the various radiometers of ARCADE. The other parts of the ARCADE instrument (loads, horns, switches, etc.) must remain at a stable temperature, but the absolute accuracy requirement is not severe because the external calibrator will calibrate all of these terms to first order. The measurement and thermal control must be performed at high altitudes ($\sim 30 \text{ km}$) while the instrument is suspended from a balloon.

In order to eliminate the reflections and emission of a window the ARCADE radiometers run without a window. The target, similar in many respects to that of FIRAS, is moved from one horn to the other to provide an external blackbody reference to compare to the sky. A blackbody internal reference reduces the dynamic range of the amplifier signal. With this arrangement, it is important to maintain the temperature of critical components in the radiometer such as the target, the internal reference, the amplifier and the horn antenna while the target is moved from one radiometer to another.

Cryogenic thermometers are often used in applications where low noise is desired and low power is required. Low level signals from the thermometers are susceptible to noise

pickup and degradation by the capacitance of long lines. Long term measurement stability is required, so it is desirable to have a thermometer system with built in calibration.

Most of the ARCADE thermometers are used to maintain thermal control of the instrument; low noise and stability are more important than knowledge of the absolute temperature. However, key thermometers are imbedded within the microwave absorber of the external calibration target. The ARCADE science goals require an isothermal target, which in turn requires precise cross calibration for the target thermometers.

II. THERMOMETER DESIGN

The system requirements include about 25 thermometers, with an $\sim 1 \text{ Hz}$ read rate, and low power dissipation, with four wire measurements. Drifts in the readout system are a concern for balloon operations so fixed resistors are included for self calibration.

RuO_2 resistive thermometers were chosen because of their low cost, long term stability, and large resistance changes in the neighborhood of 2.7 K .⁴ The thermometers are commercially available thick-film chip resistors⁵ (Fig. 1), with resistance $10 \text{ k}\Omega$ at room temperature. At 2 K , the resistance rises to $\sim 40 \text{ k}\Omega$ with a dT/dR of -0.098 , -0.158 , -1.042 , and $-10 \text{ mK}/\Omega$ at 2.2 , 2.7 , 6.3 , and 20 K , respectively. The readout noise is ultimately related to this ratio. Manganin leads ($76 \mu\text{m}$ diameter) allow four-wire resistance measurements. Mechanical stress is relieved by thermally cycling each chip 100 times between 300 and 77 K prior to soldering the leads, then another 50 times after the leads are attached. Most of the thermometers monitor the cryogenic performance of the instrument (e.g., amplifier or Dewar temperatures). The thermometers are mounted to a thin copper tab using Stycast 2850-FT epoxy, and calibrated against Na-

^{a)}Electronic mail: fixsen@stars.gsfc.nasa.gov

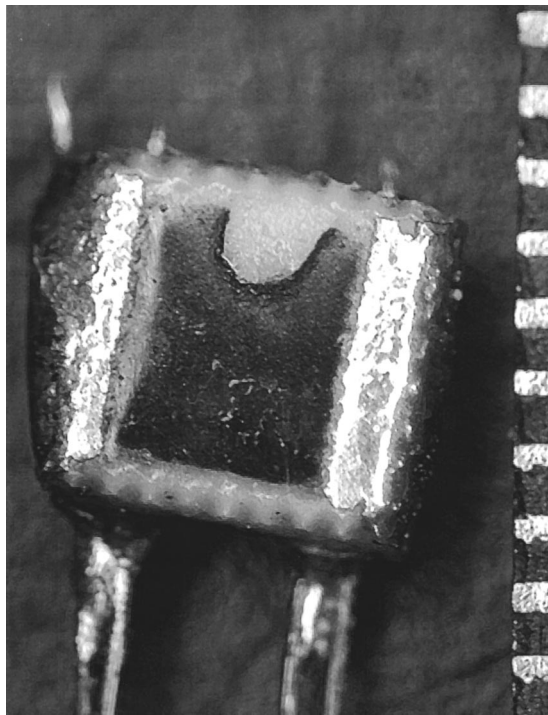


FIG. 1. RuO₂ surface mount resistor is shown. The marks on the scale are 0.01 in.

tional Institute of Standards and Technology (NIST)-traceable Ge thermometers on the cold stage of a pumped LHe Dewar.

The entire target, including five embedded thermometers, was cycled an additional ten times to relieve thermal stress, then the thermometers were calibrated *in situ* by immersing the entire target in a liquid helium bath and varying the vapor pressure above the bath. Temperature gradients within the target during calibration are small, limited ultimately by convection cells within the liquid. The absolute temperature scale is referenced to a NIST-traceable Ge thermometer and cross checked by measurement of the superfluid helium transition temperature. At temperatures near 2.7 K, the target thermometer calibration absolute accuracy is ~ 0.9 mK verified by repeated cycling and remeasurement.

The readout utilizes a four-wire resistance measurement, with an alternating excitation current and a lock-in integrator for low power and low noise.⁶ To minimize the power dissipated in the thermometer, the current is limited to $1.3 \mu\text{A}$. The readout multiplexes among 28 thermometers; the lines to each thermometer vary in length, so the line capacitance seen by the readout varies. To make each measurement in $1/30$ s and still use an alternating current to minimize the effects of offset drifts, 75 Hz was used for the excitation frequency. The circuit is shown in Fig. 2. Note that all of the

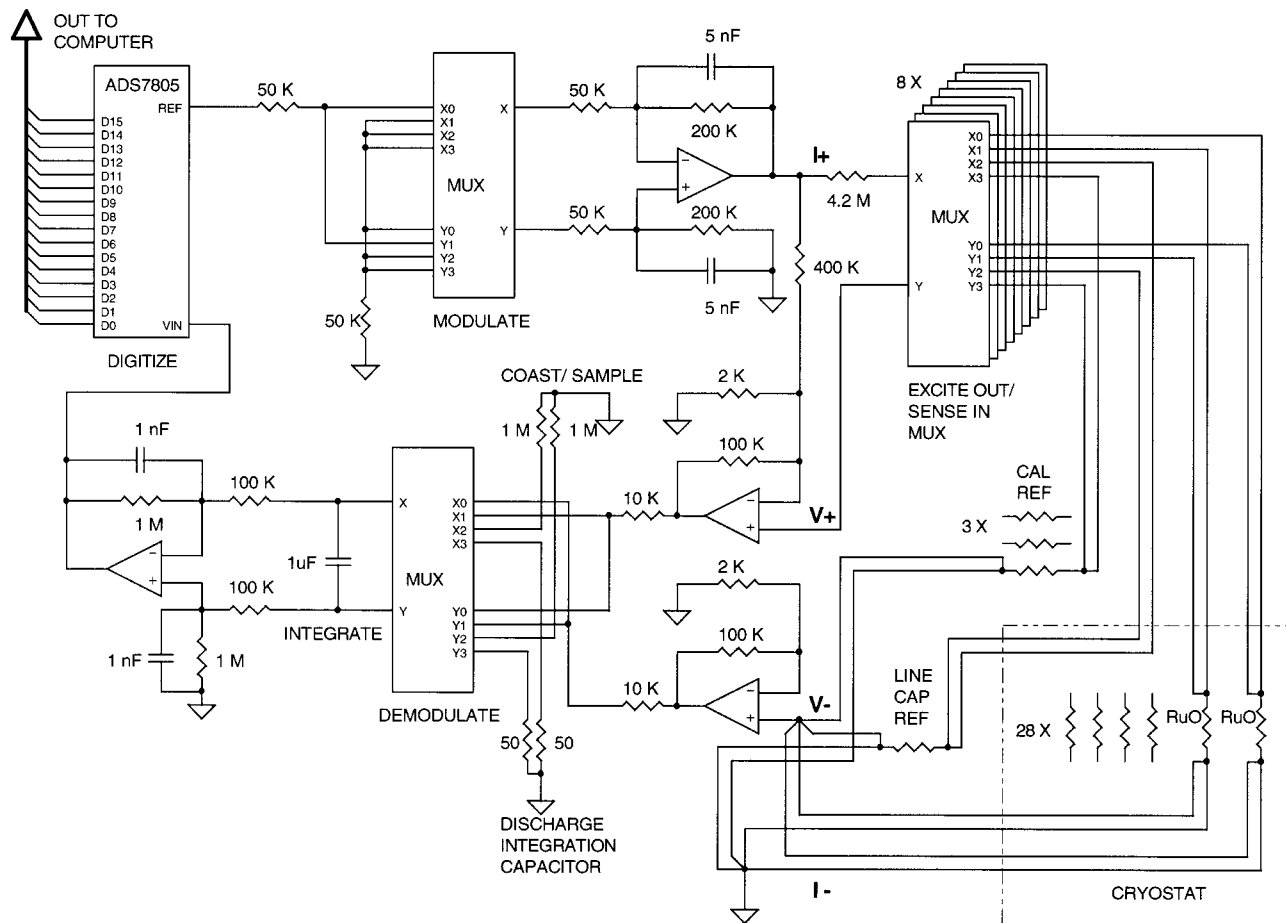


FIG. 2. Circuit diagram shows the major elements of the RuO₂ readout circuit. All of the multiplexers are CD4052 dual 4-to-1 analog multiplexers. The opamps are an LT1125 quad opamp. The integration capacitor is polypropylene for stability.

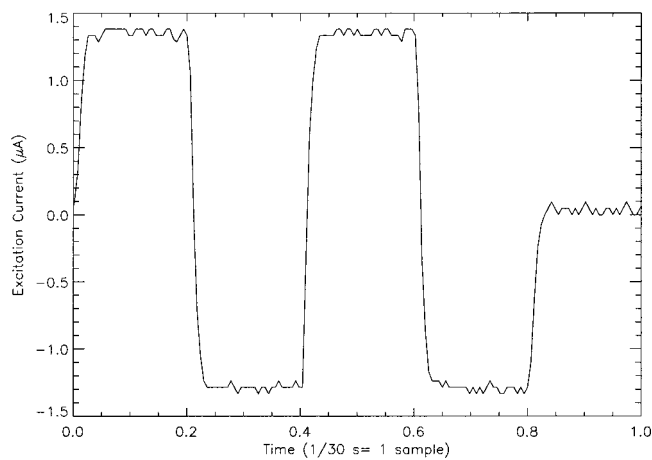


FIG. 3. Oscilloscope trace of the excitation current. The $A \rightarrow D$ converter is activated at the beginning of the fifth phase.

components except for the thermometers are maintained in a rf shielded box with a controlled temperature.

The readout of each thermometer is accomplished in five phases. Each phase is 6.7 ms long. During phases 1 and 3 the excitation current and integration signal are positive, while for phases 2 and 4 both are negative (Fig. 3). During the fifth phase the current is zero. During the first half of the fifth phase the integrator is decoupled from its input and the result is digitized. During the second half of the fifth phase the integrating capacitor is shorted to reset it for the next thermometer. At the transition from phase 5 to phase 1 the current and signal multiplexers are switched to the next thermometer (or to a reference resistor). The readout multiplexes among four calibration resistors as well as the 28 thermometers. The 32 inputs are read sequentially, and the results are sequentially relayed to a computer with RS232 protocol at 2400 Ba. The multiplexing and the off phase together reduce the duty cycle to 2.5%, so the average power dissipation is only ~ 1 nW. The same clock is used for the instrumentation phases as for the digital readout, so the time for a single sample is $1/30$ s. Thus it takes 1.067 s for a complete cycle.

The integrating capacitor is polypropylene for stability (Sprague 730P). The charging time constant is 20 ms. Low resistance discharge resistors make the discharge time constant 0.2 ms. While the signal is digitized the capacitor is essentially disconnected from any input. Figure 4 shows the signal on the integrating capacitor for five samples during a laboratory test. The digitize command (also shown) initiates the digitization at the beginning of phase 5 of the cycle just as the integrating capacitor is decoupled from the input and the current to the thermometer is zeroed.

The metal film calibration resistors were characterized: The observed change in their resistance is less than 0.5% between 295 and 77 K. The values of these resistors are distributed over the dynamic range of the RuO_2 thermometers.

III. PRINTED CIRCUIT BOARD DESIGN

To minimize the noise pickup between components, the printed circuit board was designed with internal ground and power planes. The circuit traces were distributed on the top

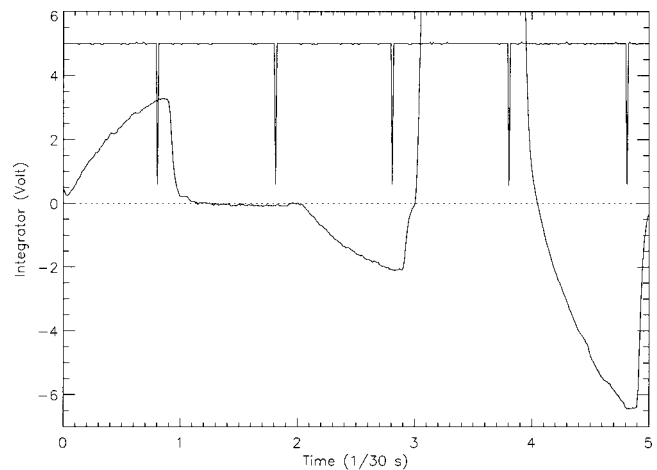


FIG. 4. Oscilloscope trace of five samples. The first sample is near 33 k Ω . The others are: 25 k Ω (the null point), 20 k Ω , open, and 10 k Ω , respectively. Also shown is the digitized command strobe.

and bottom of the board to allow for field modification of the circuit. The analog components were clustered around the opamps to keep the leads short, and the digital components were pushed to the outer edges of the circuit board to minimize their coupling into the measurement circuitry. The multiplexer chips were kept close to the input connector and the opamp to minimize line length.

IV. TESTING DESCRIPTION

During testing, the circuitry and wiring were optimized for low noise. The offset resistor, nominally 400 k Ω , was tuned to 329 k Ω to null the integrator reading at 25 k Ω (midscale or 2.7 K). Capacitance (50 pF) was added in parallel with each calibration resistor to approximately match the measured line capacitance to the sensors, and 30 Ω was added in series on each end to match the line resistance. The feedback capacitance in the excitation stage was set at 1 nF to roll off of the square wave to reduce the high frequency noise while maintaining sufficient fidelity in the square wave to avoid spikes in the demodulation. The output time constant is 0.2 ms. The cables connecting the instrument box to the dewar are 41 conductor braid-shielded cable. The shielding was grounded at both ends to minimize ground pickup noise, and the thermometer cables were separated from the cables that carry the driver lines to the ferrite switches in the instrument.

Nominally the readout voltage-to- Ω conversion is linear. For flight instrumentation and the temperature control (see Sec. V), a simple linear fit between the 20 and 25 k Ω reference resistors was used. For detailed postflight analysis calculations a second order fit was used for all four of the reference resistors. The data for the reference resistors were smoothed over 32 s intervals to minimize the noise contribution from the reference resistors. The second order fit only changes the value by a few ohms (about 1 mK).

Once the resistance was determined, the table of calibration temperatures, and resistances for each resistor, obtained in ground calibration testing, was interpolated to arrive at a

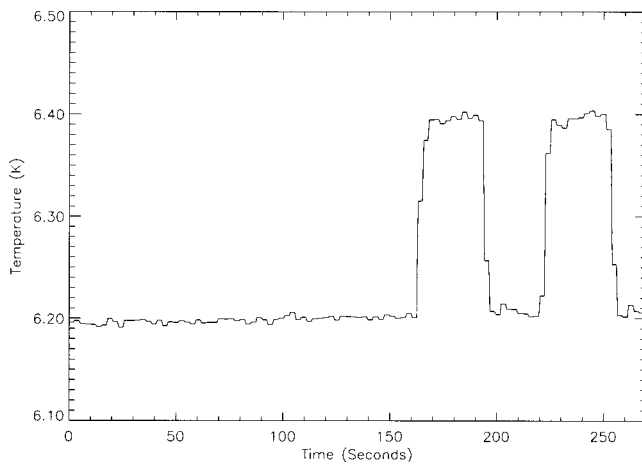


FIG. 5. 270 s of temperature data, demonstrating the control in switching between 6.2 and 6.4 K. The noise is higher at 6 K than at 2.7 K because of the dR/dT dependence on T . A careful look at the transitions shows an ~ 20 s settling time.

temperature estimate. The final uncertainty is dominated by the calibration process rather than the readout uncertainty.

V. THERMAL CONTROL

Stable temperatures of the radiometer components are required for the ARCADE science mission. To determine the coupling parameters of the radiometer to individual components, it is important to be able to change the temperature of those individual components selectively. To accomplish this, the components were placed under closed-loop thermal control.

Closed-loop thermal control was performed using (1) the temperature sensing described above, (2) a simple resistive heater driven by a $D \rightarrow A$, and (3) a software proportional-integral-differential (PID) control loop. A PID control loop imposes a restoring action proportional to the error signal (the P). In many situations this leads to oscillation so a damping term is added (the D) but an external bias leads to a long term error so an integral correction is included (the I). The signal for the control loop, in this case, was the differ-

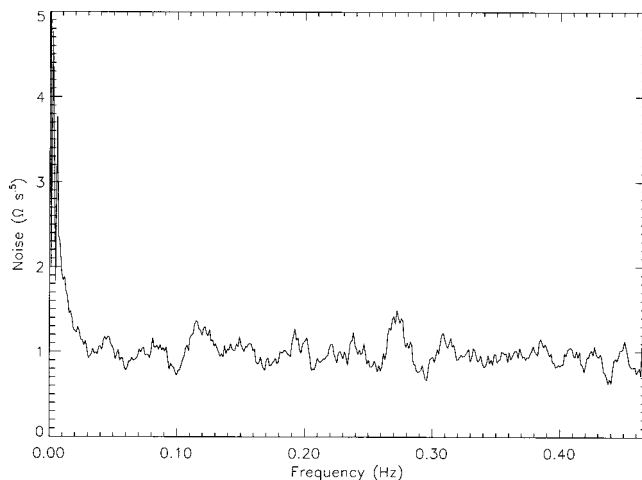


FIG. 6. Noise spectrum of one of the calibration resistors. This spectrum was taken between the relatively rare jumps of ~ 5 counts. Each count corresponds to 0.8Ω .

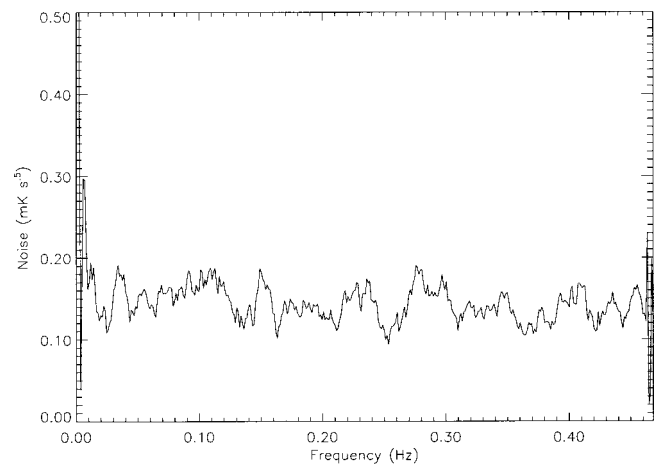


FIG. 7. Noise spectrum of one of the thermometers at 2.7 K.

ence between the measured temperature and the desired temperature (in K). The control output is calculated in watts and then converted to the appropriate value for the $D \rightarrow A$ and heater driving circuits. Ten control loops were implemented for the various instrument components.

The PID loop has an update rate of ~ 1 Hz, limited by the update rate on the temperature sensors. The PID parameters for each item to be controlled were determined empirically by using measured time constants and oscillation frequencies. The differential parameter was intentionally set to a value closer to zero than would be optimal for transient response. This allowed us to have robust control loops that do not oscillate over a wide temperature range, at a small cost in settling time after a commanded temperature change.

For each loop, only a single set of parameters was used to cover the temperature range from 2 to 20 K. Typical time constants for internal instrument components were of order 10 s. Typical control parameters were of order $k_p = 0.1$ (W/K) (proportional term), $k_i = 0.015$ (W/K s) (integral term), and $k_d = -0.02$ (W s/K) (differential term).

If the temperature error was more than a maximum value (typically 5 K), the PID loop was temporarily suspended and the heater turned full on or off. Once the temperature error was reduced to below the maximum value, PID control was restored. This loop override was useful for making quick large temperature changes. Figure 5 shows the inflight thermal control performance of the 10 GHz internal load.

VI. PERFORMANCE IN FLIGHT

Performing temperature measurement at ~ 30 km altitude puts reliability and simplicity at a premium. Care must be taken to avoid arcing (far easier at low pressure), and to make the circuit robust in the face of uncertain temperatures and launch shocks. However, the battery powered gondola has advantages as well. The circuit is far away from the 60 Hz that plagues laboratory measurements and the balloon ride is very smooth (after launch) eliminating the ground vibration. Even the air currents are light (as the balloon follows the wind), stable, and at low pressure. These together allow the inflight noise to be lower than the best measured noise in the laboratory before launch.

The four reference resistor measurements drifted only by about five counts (4Ω) over the entire flight. Most of the changes occurred in the form of discrete steps or jumps. Data near the jumps were excised. The cause of these steps was not determined although they appeared in the measurements of all of the thermometers as well. After calibration the rms noise of the measurements was $\sim 1 \Omega$ for each sample (Fig. 6). This corresponds to 0.15 mK on the RuO₂ thermometers at the critical temperature of 2.7 K, comparable to bridge measurements done in the laboratory.⁷

The final performance is shown in Fig. 7. It is not clear if the low frequency noise (below 0.02 Hz) is low frequency drift in the thermometry system or actual drifts in the temperature of the instrumented component. However, by shifting the target between the different frequency antennas every minute or so, the low frequency noise will not be an issue in measuring the cosmic background radiation at the sub-mK level.

ACKNOWLEDGMENTS

The authors would like to thank the IR Laboratory staff of the NASA/GSFC Code 685. We are also grateful to Leah Johnson, Elizabeth Cantando, and Paul Alexandre Rischard for assisting with the testing and installation during their summer program, and Anatoly Brekhman and Gary Palmer II for wiring the thermometers during their school-year internships.

¹A. Kogut, astro-ph/9607100 (1996).

²D. J. Fixsen, E. S. Cheng, J. M. Gales, J. C. Mather, R. A. Shafer, and E. L. Wright, *Astrophys. J.* **473**, 576 (1996).

³J. C. Mather, D. J. Fixsen, R. A. Shafer, C. Mosier, and D. T. Wilkinson, *Astrophys. J.* **512**, 511 (1999).

⁴W. A. Bosch, F. Mathu, H. C. Meijer, and R. W. Willekers, *Cryogenics* **26**, 3 (1986).

⁵Dale Electronic, Part RCWP-550.

⁶M. R. Corson, *Rev. Sci. Instrum.* **56**, 2310 (1985).

⁷E. Baciocco, C. Boragno, and U. Valbusa, *Cryogenics* **29**, 209 (1989).